SSN 97.21
Task 8.118

CONF-970465--19

BNL-64388

Application of Resonance Raman Lidar for Chemical Species Identification *

Carl L. Chen, Daniel L. Heglund, Mark D. Ray, David Harder, Ronald Dobert,
King P. Leung, Ming Wu and Arthur Sedlacek
Brookhaven National Laboratory, Upton, NY 11973

Abstract

BNL has been developing a remote sensing technique for the detection of atmospheric pollutants based on the phenomenon of resonance Raman LIDAR that has also incorporated a number of new techniques/technologies designed to extend it's performance envelope. When the excitation frequency approaches an allowed electronic transition of the molecule, an enormous enhancement of the inelastic scattering cross-section can occur, often up to 2 to 4 orders-of-magnitude, and is referred to as resonance Raman (RR), since the excitation frequency is in "resonance" with an allowed electronic transition. Exploitation of this enhancement along with new techniques such as pattern recognition algorithms to take advantage of the spectral fingerprint and a new laser frequency modulation technique designed to suppress broadband fluorescence, referred to as Frequency Modulated Excitation Raman Spectroscopy (FreMERS) and recent developments in liquid edge filter technology, for suppression of the elastic channel, all help increase the overall performance of Raman LIDAR.

Introduction:

Brookhaven National Laboratory (BNL) has been tasked to examine and improve upon the performance of Raman spectroscopy-based lidar platforms. This multi-year effort has resulted in the fabrication and field testing of two state-of-the-art Raman lidar platforms. The reason that Raman lidar is so valued as a pollution sensors originates from some of the advantages[1-6] that a Raman-spectroscopy offer, namely: (1) very high selectivity (chemical specific fingerprints), (2) independence from the excitation wavelength (ability to monitor in the solar blind region), (3) chemical mixture fingerprints are, to first order, the sum of its individual components (no spectral cross-talk), (4) near independence of the Raman fingerprint to its physical state (very similar spectra for gas, liquid, solid and solutions), and (5) insensitivity of the Raman signature to environmental conditions (no quenching, or interference from water). The detection of atmospheric components using Raman backscattering of laser radiation dates back to the pioneering work of Leonard[7] in 1967. In that study, he used a pulsed N_2 gas laser at 337.1 nm to generate Raman return signals from N_2 and O_2. Further investigations during the early 1970s pushed the envelope of performance for a Raman LIDAR.[8-11] However, due to the lack of tunable UV laser sources, these early investigations were not able to take advantage of near-resonance enhancement of the Raman cross-section which occurs when the excitation frequency approaches an electronically excited state of the molecule[1,12-16]. The enhancement of the scattering cross-section can be quite large, often approaching 2 to 4 orders of magnitude. This improvement in the cross-section, in conjunction with the global advantages of Raman spectroscopy cited earlier and the availability of frequency-tunable, all solid-state UV laser systems and high-sensitivity/low-noise array detectors, provides a promising optical platform for the remote open-path atmospheric sensing.

Experimental:

Since the specifics concerning the acquisition of Raman and resonance Raman return signals has been documented elsewhere[17], only those issues relating to the details of the two units (a 48' long x 13' high x 8' wide trailer and a 33' long van) under evaluation at Brookhaven will be discussed here. The BNL resonance Raman chemical sensor is typical of most Raman LIDAR configurations. The two platforms are composed of three main subsystems: (*i*) a laser system and beam transport optics, (*ii*) signal receiver telescope and spectral fingerprinting detection unit, and (*iii*) equipment control and data acquisition/processing subsystem. In the case of the main trailer unit, the laser source is a frequency agile laser system (Spectra-Physics 730 MOPO system) whereas the van is a single frequency 266 nm Nd:YAG laser (Coherent Infinity). All timing aspects of each

==========

*Work performed under the auspies of U.S. Department of Energy, Contract DE-AC02-76CH00016.

DISCLAIMER

system are based on a single master oscillator which provides triggering to the laser and gate delay timing to the detector circuitry.

For the trailer system following the laser trigger from the master oscillator, the 6 mm diameter, 270-560 nm laser beam (of 3-4 ns duration) was expanded to a diameter of 100 mm via a 1:16 beam expander prior to exiting the trailer. The return signals were collected by an effective 27-inch Cassegrain telescope and focused onto the slits of a single grating spectrometer (1200 grooves/mm) and then detected by an Oriel's Intaspec V intensified CCD (charge-coupled device) camera for spectral fingerprinting. For the lidar system in the van, the laser wavelength is fixed at 266 nm, and the receiver telescope is 16-inches in diameter. All other features are the same as that described for the trailer. In order to avoid the possibility of charge saturation of pixels by the unwanted Rayleigh-return, and to prevent charge spill-over to the Raman channels, a Brookhaven fabricated knife-edge filter was employed for the preferential removal of the Rayleigh signal return.

Results and Discussion:

Figure 1 displays the Raman return signals collected during a release of nitrobenzene. As can be clearly seen in the figure the presence of nitrobenzene is unambiguous and clearly discernible against the background. In addition to collecting a vibrational fingerprint from the interrogated

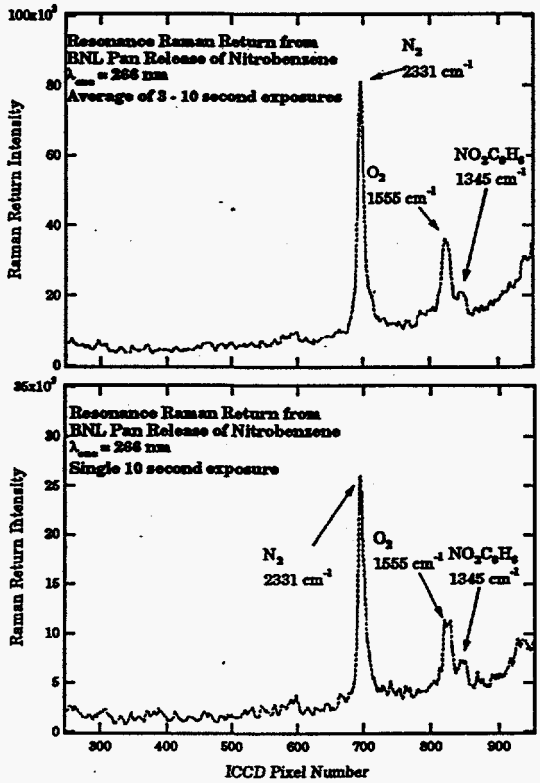

Figure 1: Raman Return Signals at 0.5 km

chemical plume, the resonance Raman chemical sensor has the other distinct advantage that every spectra collected will also contain return signals from atmospheric nitrogen and oxygen, therefore providing a self-calibration of the plume concentration with return-signal intensities.[1-16] This concentration self-calibration is accomplished by comparing the integrated areas under the respective return signals for the knowns (N_2 and O_2) and the unknowns (in the present case nitrobenzene), and using their respective scattering cross-sections. The Raman scattering cross-sections for these two atmospheric species as a function of laser excitation wavelength is well documented in the literature[15]. For the specific case of NO_2-C_6H_5 the resonance Raman scattering cross-section as a function of excitation wavelength has been measured by Ahmad and co-

workers.[18] For laser excitation at 266 nm, the resonance Raman scattering cross-section is estimated to be on the order of 2 x 10^{-26} cm^2/sr. In order to insure accuracy of the field measurements the N_2-to-O_2 return signals can also be used to provide an estimate of atmospheric absorption effects. This is accomplished by exploiting the fact that the nitrogen-to-oxygen ratio in the troposphere is a constant, therefore any deviation would provide a DIAL-like measure of the atmospheric absorption. This application of the N_2 to O_2 return-signals was pioneered by Renaut and Capitini in the 1980s.[19] The respective areas under the N_2, O_2 and NO_2-C_6H_5 return signals were calculated assuming a Voigt lineshape for the Raman bands. By using the known concentrations, measured integrated signals, and their respective scattering cross-sections, it is estimated that the nitrobenzene concentration for the signal shown in Figure 1 was ~ 40 ±20 ppm.

Since resonance Raman spectroscopy requires an allowed electronic transition, the potential exists for concomitant photon emission through the fluorescence channel, which, if strong enough, can mask the structured Raman spectral fingerprint. Furthermore, during daytime remote chemical sensing, background solar irradiance can also obscure weak spectral signatures in the return signal. Therefore, a technique is needed which can either suppress or eliminate this unwanted background signal without distorting the underlying Raman spectral fingerprint. Additionally, this technique should also be robust enough for use with any chemical species or chemical mixture, without becoming increasingly technically prohibitive to implement. Unfortunately, the LIDAR remote sensing scenario effectively precludes many of the well-known laboratory-based techniques for fluorescence and/or background suppression (i.e., addition of fluorescence quencher). In an effort to address this problem, Brookhaven National Laboratory is developing a technique based on the modulation of the excitation frequency (wavelength) which does not require phase-sensitive, lock-in detection and which can exploit the advantages of multichannel detection for full Raman spectrum collection for every excitation laser pulse. This technique is called Frequency Modulated Excitation Raman Spectroscopy or simply FreMERS.

The origin for this idea can be traced back to the results of Mathies and co-workers[20] in 1992. In that study, an Ar^+ laser pumped Ti:sapphire laser (tunable from ~ 670 nm to 1100 nm) was used and Raman-plus-fluorescence spectra collected at two, slightly different (5-10 cm^{-1}) excitation wavelengths. For such small changes in the excitation wavelength, the assumption that the fluorescence will not change appreciably over the wavelength range becomes less of a limiting condition. Therefore, by taking the difference of two Raman-plus-fluorescence signals collected at two slightly different excitation wavelengths, a fluorescence-free Raman spectrum can be generated. This fluorescence-free spectrum will look like a first derivative signal. By examining the Raman spectra from chloroform in various amounts of laser dye, Mathies and co-workers[20] were able to detect Raman return in samples where the fluorescence was 1000 times larger. We have extended this technique to the visible and ultraviolet spectral regions and to pulsed laser systems. In addition, we are also developing a variation of this technique which requires only a single excitation wavelength for background reduction as opposed to two excitation wavelengths, thereby greatly reducing the required time for data acquisition and minimizing the complex data reduction schemes otherwise necessary in order to correct for the effects of atmospheric turbulence at two wavelengths.

In Figure 2 the experimental proof-of-principle of FreMERS is shown for a sample of 25,000 ppm of carbon tetrachloride in a laser dye. The original signals are shown along with the generated FreMERS spectrum. The upper two traces labeled "a" and "b" are the Raman-plus-fluorescence signals at two excitation laser wavelengths, offset for clarity, separated by a small wavelength difference ~0.3 Å. This value of the wavelength shift, determined experimentally, is on the order of half the expected Raman linewidth. Right below trace "b" is the FreMERS signal, labeled trace "c". Numerical integration of the resulting FreMERS spectrum is shown in trace "d". The Raman spectrum of pure carbon tetrachloride is reproduced here as trace "e" for reference. As can be clearly seen, the FreMERS technique was able to extract the carbon tetrachloride Raman signal from high background without any major spectral degradation. This experiment represents the successful extraction of a Raman signal that is 1/1000 the size of the fluorescence background.

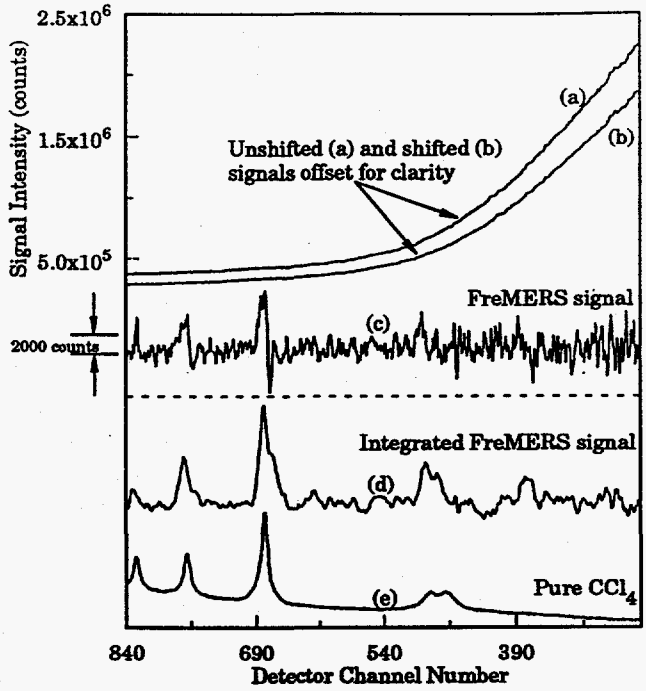

Figure 2: 25,000 ppm of carbon tetrachloride in a laser dye. Top signals (a & b) are the Raman-plus-fluorescence signals, and below are the resulting spectral FreMERS signal (c), the numerical integration of the FreMERS signal (d) and a Raman spectra of pure carbon tetrachloride for reference.

Justification of this background suppression procedure can be seen by the following model, which assumes that Raman lines are Gaussian-like. Within this approximation, the Raman-plus-fluorescence spectrum of a molecule can be represented mathematically as

$$S_{r+f} = P(\lambda)\left[F(\lambda)+R(\lambda)\right] = P(\lambda)\left[F(\lambda)+\frac{1}{\sqrt{2\pi}}\sum_{i=1}^{N}\frac{A_i}{\sigma_i}\exp\left[\frac{-(\bar{\nu}-\bar{\nu}_{oi})^2}{2\sigma_i^2}\right]\right], \qquad (1)$$

where each Raman-plus-fluorescence signal is identified by N Gaussian-like Raman peaks, each of which is characterized by area A_i, a center position $\bar{\nu}_{oi}$, a standard deviation σ_i, and the background fluorescence signal itself, $F(\lambda)$. The term $P(\lambda)$ accounts for the individual responsivity of each pixel on the multichannel detector. By keeping the monochromator at the same spectral setting, this pixel responsivity can be eliminated. The generation of a FreMERS signal involves the subtraction of two successive Raman-plus-fluorescence signals, collected at two slightly different excitation wavelengths (λ and $\lambda + 1/\delta$), where δ is on the order of a few wave numbers, and which can be expressed within this mathematical framework as

$$\text{FreMERS}(\bar{\nu}) = \frac{1}{\sqrt{2\pi}}\sum_{i=1}^{N}\frac{A_i}{\sigma_i}\left\{\exp\left[\frac{-(\bar{\nu}-\bar{\nu}_{oi}+\delta)^2}{2\sigma_i^2}\right]-\exp\left[\frac{-(\bar{\nu}-\bar{\nu}_{oi})^2}{2\sigma_i^2}\right]\right\} \qquad (2)$$

Since δ is very small, $F(\lambda) \approx F(\lambda + 1/\delta)$, the fluorescence background is removed by this process as evidenced in Figure 2. This will be investigated further by conducting a series of experiments where δ is changed incrementally and examining the behavior on the FreMERS signal. It is expected that,

with an 18-bit dynamic range of the detector, detection limit approaching 1/10,000 the size of the background can be achieved.

In addition to the requirement of dealing with potential interferences from the fluorescence channel, there also exists a need for better suppression of the elastic channel (Rayleigh & Mie scattering) so that lower frequency modes of molecules of interest can be exploited. The development of super-notch filters provided a giant leap forward, but due to material science issues these filters have been limited in their use to the visible and near-IR spectral regions. This limitation meant that in order to suppress this channel in the near-UV and UV spectral regions, one was limited to either a knife-edge filter or the dispersion provided by a double or even a triple - grating spectrometer. Very recently however, Harris and co-workers[21] have demonstrated a series of easily fabricated liquid edge filters useful down to approximately 288 nm. These liquid filters allow vibrational modes as low as 200 - 300 cm^{-1} to be observed, thus opening up a new vibrations for spectral fingerprinting. Field experiments will be commencing soon where these liquid edge filters will be evaluated as to their utility with Raman lidar.

In an effort to take advantage of the Raman spectral fingerprints, Brookhaven has been pursuing the development of pattern recognition algorithms. Of partial interest has been the development of an adaptive mixing (AM) algorithm which has several advantages over artificial neural networks and partial least squares algorithms when used in atmospheric LIDAR. One special feature of the AM algorithm is its ability to use only one neat spectrum per chemical for chemical mixture identification, and hence greatly minimize the required training. This is in contrast to the conventional neural-net pattern recognition technique(s) which usually require a large number of field spectra, noise and all, for training. The large number of data set pertains to different field conditions. Since typical field data are time consuming and usually difficult to obtain, that is why the AM algorithm stands out as a simple and elegant method in comparison with the other algorithms such as Partial Least Squares (PLS)[22, 23] and Classical Least Squares (CLS).[24] In both cases, AM algorithm can provide a more flexible frame work to accommodate diverse physical constraints.

For field data analysis, it is important to be able to pre-process the spectral data removing the artifacts, but retaining the spectral fingerprints, prior to chemical identification. For example, LIDAR artifacts such as Rayleigh scattering, self absorption, turbulence and speckle can greatly influence the detection and recognition accuracy. Especially when these noise sources produce amplitude response of the detector system equal to or larger than the weaker spectral components of interest. In this case, special pre-processing technique(s) can help bringing out the weak chemical fingerprints. Application of the AM algorithm to the detection of similar chemicals with concentration differences approaching as high as 799:1, in both neat and noisy conditions demonstrate the large dynamic range potential of this technique.

The motivation to develop a simple algorithm to overcome the nonlinearities presented in the neural net approach Multi-Layer Perceptron (MLP's), is to find a reliable method which can analyze mixtures with highly disproportion concentrations. The adaptive mixing (AM) algorithm is therefore developed for solving this potential problem, and the algorithm is tested with the following exercise.

A simulated mixture spectrum is first constructed by summing prototype spectra from the neat chemical spectral database. Each prototype spectrum has a corresponding weight representing its contribution to the total spectrum, initially set to zero. A fitness measure is then made by examining the squared Euclidean norm between the true and the simulated mixture spectrum. Weights of each database spectrum are changed sequentially by a fixed step until no further reduction in the total error can be obtained. The same procedure is then repeated by using progressively smaller increments of weight correction until the total residual error is below a predetermined threshold (based on the user's assessment of database completeness and normalization accuracy considerations) and the process is halted. At this point the normalized weights for each chemicals are output as the best estimate for the mixture coefficients. If the residual error cannot be reduced below the predetermined threshold, AM will assume that one or more out-of-database chemicals are present and report this finding to the user. The AM logic is presented as follows:.

The ith chemical spectrum in a database of m chemicals is defined as S(i,j), j= 1:m, where i indicates the m spectral samples from 1:m. A mixture of n-chemical mixture spectrum is defined as:

$$M(j) = \sum_{i=1}^{n} W(i) * S(i, j) \tag{3}$$

Initially W(i) = 0 for all 1<=i<=n. For an unknown mixture spectrum of U(j), j=1:n, the fitness or error measure E is defined by:

$$E = \sum_{j=1}^{M} [U(j) - M(j)]^2 = \sum_{j=1}^{M} [U(j) - \sum_{i=1}^{N} [W(i) * S(i, j)]]^2 \tag{4}$$

For n=1 the value W(1) is repetitively increased by a fixed value Δ until no further decrease in E is obtained. The value W(1) is then fixed. W(2) through W(n) are adjusted similarly, fixing the value W(n) when no further error reduction is possible.

After this first cycle of estimation, the fixed increment Δ is then reduced by a factor of 10 (i.e. Δ = Δ * 0.1). The above process is repeated for W(1) through W(N) until no further reduction of error is possible. Error reduction is accomplished by immediately adjusting each W(i) before W(i+1).

The process is repeated several times, using a factor of ten smaller Δ each cycle from the previous iteration. The process converges rapidly after a small number of iterations, typically about five or six. Each cycle, the values of W(i) are normalized so that their sum from i=1:n is equal to unity. The final set of W(i) are saved, and their values are best estimates of the component chemicals.

We have tried this algorithm on a simulated mixture with 1000:1 concentration ratio and with progressively larger values of noise. Clean spectra of trichloromethane and toluene were used to simulate the mixture spectrum composing of 99.9% trichloromethane and 0.1% toluene. Gaussian noise with increasing amplitude distribution were added to the mixture until S/N =1.0 was obtained -- relative to the smaller component. We found that for S/N=1.0 the concentration estimates for trichloromethane and toluene were 0.999± 0.0003 and 0.001± 0.0003, respectively. The absolute error is constant, i.e., 0.0003, but the relative error is progressively higher for the lesser component, in this case 30 percent.

Both Partial Least Squares (PLS)[22, 23] and Classical Least Squares (CLS)[24] can be used to directly compute the mixture coefficients in a LIDAR return signal. Though PLS works best when multiple spectra for each chemical are used in training, it can be trained with a "single" spectrum per chemical. In fact, CLS works this way, using a single spectrum to represent each chemical in the database. Iterative methods such as the AM algorithm and similar methods appear to find the same mixture coefficients, however at greater computing time. Our results show that CLS performs at the same level of accuracy as AM, though execution is faster in CLS, since it requires only one matrix algebra step. AM, however, is able to incorporate diverse constraints, which can not be done in CLS. One example of diverse constraints is limitation of the estimated vectors to be within a special region of space, hence quadratic.[26] CLS and PLS are in the category of what are commonly known as *unconstrained* optimization[26], i.e. they search the *entire space* of both positive and negative mixture coefficients.

Unconstrained optimization, though perhaps more computationally efficient, is not physically meaningful unless absorptive processes are involved. In a typical scattering scenario one normally requires that the derived mixture coefficients are non-negative. Furthermore, since no finite database can ever be complete to cover all chemicals, one needs to deal with the situation where an *unknown* chemical may be present.

Conclusions and Prognosis:

We have discussed recent experimental results using a resonance Raman based LIDAR system as a remote pollution sensor. This spectroscopy has the fundamental advantage that it is based on optical fingerprints that are unique to each molecular species and are insensitive to environmental perturbations or excitation frequency. By taking advantage of resonance enhancement, the inelastic scattering cross-section can increase anywhere from 2 to 4 orders-of-magnitude translating into increased sensing range or lower detection limits. The availability of frequency-agile UV lasers, high-gain\low-noise multichannel detectors and other state-of-the-art technologies now allows the phenomenon of resonance-enhanced Raman spectroscopy to be fully exploited as a remote chemical sensor platform. Since many chemicals have electronic transitions in the UV/VIS, it is expected that many will have pronounced resonance enhancements. In addition, a new technique designed to suppress the broadband fluorescence, should it accompany the resonance Raman signal was also presented. We have demonstrated that the Adaptive Mixing algorithm is able to accurately detect chemical mixture spectra which are contaminated by noise and distortion. Accuracy exceeding 98 percent have been observed on highly similar o-, m-, and p-xylene spectra having S/N ratios of 1:1 and (molar) concentration ratios of 799:1. Simulated multi-peak spectra are correctly detected with an accuracy of 94.2 percent at the same S/N ratio. These results extend to the more difficult problem of single-peak chemical fingerprints. Detection accuracy of 88 percent at S/N ratio of 3:1 was obtained.

References:

1. Measures, R. M., Laser Remote Chemical Analysis, in *Chemical Analysis Series Vol. 94*, R. M. Measures, Ed., John Wiley and Sons: New York 1988.
2. Hendra, P., Jones, C. and Warnes, G., *Fourier Transform Raman Spectroscopy: Instrumentation and Chemical Applications*, Ellis Horwood: New York 1991.
3. Grasselli J. G. and Bulkin B. J., *Analytical Raman Spectroscopy*, John Wiley and Sons: New York 1991.
4. Carey, P. R., *Biochemical Applications of Raman and Resonance Raman Spectroscopies*, Academic Press: New York 1982.
5. Schrötter, H. W. and Klöckner H. W., Raman Spectroscopy of Gases and Liquids in *Topics in Current Physics*, A. Weber, Ed., Springer-Verlag: New York 1979.
6. Long D. A., *Raman Spectroscopy*, McGraw-Hill: New York 1977.
7. Leonard, D. A., Nature **216**, 142 (1967).
8. Kobayasi, T and Inaba, H, Opto-Electron. 2, 45 (1970);Kobayasi, T and Inaba, H, Proc. IEEE **58**, 1568 (1970).
9. Inaba, H and Kobayasi, T, Opto-Electron. 4, 101 (1972).
10. Melfi, S. H, Lawrence, J. D. and McCormick M.P.M., Appl. Phys. Lett. **15**, 295 (1969)
11. Melfi, S.H., Appl. Opt. **11**, 1605 (1972).
12. For example see: Penny, C.M., Morey, W.W., St. Peters, R. L., Silverstein, S.D., Lapp, M., and White, D.R., NASA Report, **NASA-CR-132363**, Sept. 1973:Penny, C.M and Silverstein, S.D. General Electric Report, **GE-72CRD150**, May 1972.
13. Rosen, H, Robrish, P., and Chamberlain, O., Appl. Opt. **14**, 2701 (1975).
14. Rousseau, D. L., Friedman, J. M. and Williams, P. F., Raman Spectroscopy of Gases and Liquids in *Topics in Current Physics*, A. Weber, Ed., Springer-Verlag: New York 1979.
15. Asher, S. A., *Ann. Rev. Phys. Chem.* **39**, 537 (1988).
16. Ziegler, L. D. and Albrecht, A. C., J. Chem. Phys. **70**, 2634 (1979).
17 Chen, C. L. and Sedlacek, A. J., Sedlacek, Ed., SPIE Proc. Vol 2833, p 182 (1996).
18. Ahmad, S. R. and Foster, V. G., Sedlacek, Ed., SPIE Proc. Vol 2833, p 105 (1996).
19. Renaut, D., Pourny, J.C., and Capitini, R., J. Atmos. Ocean. Tech. **5**(5) 585 (1988); Renaut, D., Pourny, J.C., and Capitini, R., Optics Lett. **5**, (6) 233 (1980)
20. Shreve.,A. P., Cherepy, N.J. and Mathies, R.A., Appl. Spectro. **46**(4) 707 (1992).
21. Kleimeyer, J. A.,, Fister, J. C., Zimmerman, J., and Harris, J.M., Appl. Spectro. **50** (12) 1597 (1996).
22. D. Haaland and E. B. Thomas, Anal. Chem. 60, 1193, 1988.
23. D. Haaland and E. V. Thomas, Anal. Chem. 60, 1202, 1988.
24. W. H. Press, et al, Numerical Recipes in C, Cambridge University Press, New York, 1988.
26. William Conaway, Lawrence Livermore National Laboratory, private communication, 1996.